scientific reports

Check for updates

OPEN

HSD17B1-mediated trophoblast differentiation lowers estrogen levels in early-onset preeclampsia

Shu Zheng[1], Wei Feng[2], Zewen Sun[2], Peng Xu[1], Shuai Dong[1], Lin Pan[3], Huimin Shen[1], Jin He[1], Peng Chen[2]✉ & Chang Shu[1]✉

Early-onset preeclampsia (EOPE) with fetal growth restriction (FGR) is a severe hypertensive disorder of pregnancy characterized by placental dysfunction and estrogen deficiency. Based on single-cell RNA sequencing (scRNA-seq) profiling of specific placental trophoblast subtypes from EOPE-FGR and normotensive pregnancies, we identified *HSD17B1*, which encodes a key enzyme mediating estradiol conversion, as the central dysregulated node in EOPE pathogenesis. Multi-modal computational analysis (cluster annotation, cellular proportion calculation, comparison of differentially expressed genes, and characterization of cellular developmental trajectories) revealed key expression dynamics during syncytiotrophoblast (SCT) differentiation, with substantial suppression in EOPE specimens. Further validation using clinical placental samples confirmed the downregulation of HSD17B1 at the protein level in patients with EOPE, as demonstrated by immunohistochemistry and western blotting. Mechanistically, *HSD17B1* knockdown in BeWo trophoblast models recapitulated the core EOPE phenotypes of impaired SCT differentiation and estrogen biosynthesis blockade. These findings reveal that HSD17B1 is a master coordinator of trophoblast-endocrine crosstalk, the impairment of which in placental trophoblasts may contribute to EOPE pathogenesis. Our findings provide a mechanistic basis for developing HSD17B1-targeted interventions that could contribute to the concurrent restoration of placental competence and hormonal regulation, improving the perinatal outcomes of patients with EOPE.

Keywords Early-onset preeclampsia, Estrogen, Biomarkers, Single-cell RNA sequencing, Syncytiotrophoblast, Differentiation

Early-onset preeclampsia (EOPE), a severe hypertensive disorder of pregnancy affecting 1–2% of pregnancies globally, represents a multifaceted syndrome marked not only by placental dysfunction but also by increased oxidative stress, inflammation, and metabolic dysregulation[1–3]. These interconnected pathological processes create a self-perpetuating cycle of endothelial damage and systemic vascular dysfunction, imposing disproportionate burdens on maternal cardiovascular systems and fetal development[4,5]. Fetal growth restriction (FGR), a pathognomonic manifestation of placental insufficiency, frequently coexists with EOPE, wherein over 60% of cases are characterized by villous maldevelopment and impaired trophoblast invasion[6,7]. Notably, while EOPE is predominantly driven by placental maldevelopment and abnormal trophoblast invasion, late-onset preeclampsia (LOPE) is more often associated with pre-existing maternal metabolic and vascular disturbances[8]. Thus, EOPE serves as a more direct model for investigating placenta-specific mechanisms of preeclampsia. The placenta orchestrates multifaceted physiological processes, including nutrient and oxygen exchange, immune tolerance, and hormone production, with emerging evidence highlighting the vital role of estrogenic signaling in maintaining a healthy pregnancy. Estrogen plays an essential role in regulating vascular health, modulating immune responses at the maternal–fetal interface, and supporting placental development. Notably, EOPE placentas are characterized by pronounced disruptions of estrogen signaling associated with fetal malperfusion and adverse perinatal outcomes[9,10]. Consequently, investigating the molecular nexus between the disruption of estrogen signaling, placental dysfunction, and EOPE is essential for the development of targeted EOPE interventions.

[1]Department of Obstetrics, Obstetrics and Gynecology Center, The First Hospital of Jilin University, Jilin University, Changchun 130021, China. [2]Department of Genetics, College of Basic Medical Sciences, Jilin University, Changchun, China. [3]The First Hospital of Jilin University, Jilin University, Changchun 130021, China. ✉email: pchen@jlu.edu.cn; shu_chang@jlu.edu.cn

The hydroxysteroid (17β) dehydrogenase (HSD17B) enzyme family comprises bioactive steroid gradient regulators, which play pivotal roles in regulating the bioavailability of estrogen and androgen during pregnancy[11]. These enzymes catalyze tissue-specific interconversions between active 17β-hydroxysteroids (e.g., estradiol [E2]) and their inactive forms (e.g., estrone [E1]), spatiotemporally tuning hormonal signaling during pregnancy[12]. Among the 15 known human HSD17B isoenzymes, HSD17B1 has been identified as the principal estradiol synthase that promotes the conversion of E1 to bioactive E2, the latter of which is characterized by a stronger affinity for estrogen receptors and is essential for sustaining placental function throughout pregnancy[13,14]. The complementary steroid regulatory roles of these enzymes are exemplified by HSD17B2-mediated estrogen inactivation (E2→E1) and HSD17B3-driven androgen biosynthesis (androstenedione→testosterone), highlighting the functional diversification of these dehydrogenases in hormonal homeostasis[11,15,16]. Given its bottleneck status in estrogen biosynthesis, HSD17B1 is considered to function as a central regulator of placental–endocrine crosstalk, in which changes in its activity and expression can profoundly influence pregnancy outcomes.

However, despite the pivotal role of HSD17B1 in placental steroidogenesis, its expression dynamics among different trophoblast differentiation states and the primary causes of placental dysfunction in EOPE-associated FGR have yet to be sufficiently determined. Furthermore, the mechanistic hierarchy between HSD17B1 downregulation and trophoblast maldifferentiation (syncytialization defects and hormonal imbalance) remains unclear, thereby impeding the identification of therapeutically tractable nodes in the EOPE-associated pathogenic cascade. However, emerging single-cell RNA sequencing (scRNA-seq) technologies have revolutionized our analysis and understanding of placental cellular heterogeneity, facilitating the identification of previously unrecognized trophoblast subpopulations with specialized endocrine functions and EOPE-associated pathways[9,17,18]. These advances highlight the necessity of cellular-resolution interrogation to establish the regulatory roles played by HSD17B in the placental ecosystem.

To investigate the cellular and molecular mechanisms underlying EOPE pathogenesis, we employed single-cell transcriptomic profiling of placental tissues derived from patients with EOPE and normotensive pregnancies. Our results revealed that the estrogen-related gene *HSD17B1* is a central regulatory hub governing both SCT and estrogen homeostasis. In addition, transcriptomic and clinical analyses revealed the predominant expression of HSD17B1 in the SCT subpopulation, with pronounced downregulation in EOPE specimens. Mechanistically, *HSD17B1*-silenced trophoblast models have revealed that *HSD17B1* plays a dual regulatory role in estrogenic amplification and trophoblast differentiation. These findings provide evidence that the low estrogen levels observed in EOPE may be associated with both a direct deficiency of HSD17B1 enzymatic activity and the indirect effects of impaired SCT differentiation. Our findings in this study establish HSD17B1 as a nodal regulator at the crossroads of trophoblast development and endocrine signaling, providing valuable insights into EOPE pathogenesis and a potential framework for precision interventions.

Results

scRNA-seq profiling and cell typing of placental tissue from patients with EOPE with FGR and healthy pregnancies

To achieve a comprehensive understanding of the cellular heterogeneity within the human placenta, placental parenchymal biopsies were collected from specific regions of two placentas: one from a patient with EOPE and the other from a healthy pregnant woman. Both were obtained immediately after delivery via cesarean section. The tissues were processed, dissected, and enzymatically digested to generate single-cell suspensions, which were subsequently analyzed using scRNA-seq on a 10× Genomics Chromium platform. Data analysis was performed to assess the transcriptional profiles and cellular composition across samples[19] (Fig. 1a). In total, 17,526 high-quality cells from both samples were included in the analysis. Cellular composition was examined using principal component analysis (PCA) with unbiased clustering across all cells, and the results were visualized using Uniform Manifold Approximation and Projection (UMAP) (Fig. 1b, c). Twelve main clusters were identified based on cluster-specific marker genes (Supplementary Table S1) using DEG analysis. These clusters included B cells, decidual cells, endothelial cells, erythroblasts, fibroblasts, macrophages, mast cells, monocytes, neutrophils, natural killer cells, T cells, and trophoblasts (Fig. 1d). Clustering revealed a remarkable diversity of cell types, with placental trophoblasts prominently located in major clusters at the bottom of the UMAP plot.

A substantial proportion of trophoblasts (3,899; 22.25%) was categorized into three subgroups: extravillous trophoblasts (EVTs), villous cytotrophoblasts (VCTs), and SCTs[20]. During trophoblast differentiation, VCTs act as progenitor cells that either fuse to form a multinucleated SCT cell layer or undergo epithelial-mesenchymal transition to become EVT cells. SCTs, which form the outer layer of the placental villi, serve as primary sites for gas and nutrient exchange between the mother and the fetus[21]. They also secrete hormones to protect the fetus from pathogens[22]. In contrast, EVT cells are migratory and invasive and play a key role in placental implantation and fetal development[23,24] (Fig. 2a).To further characterize these trophoblast clusters, VlnPlot and FeaturePlot were used to analyze the expression patterns of their respective marker genes (Fig. 2b, c). Placental EVTs express non-classical forms of HLA, such as *HLA-G*, to promote maternal–fetal immune tolerance by modulating uterine natural killer cells[25]. Additionally, pappalysin 2 (*PAPPA2*) a pregnancy-associated metalloproteinase expressed specifically in extravillous trophoblasts (EVTs), cleaves insulin-like growth factor binding proteins to enhance IGF bioavailability, thereby promoting trophoblast invasion and placental vascular remodeling[26]. PAGE Family Member 4 (*PAGE4*) and Paternally Expressed Gene10 (*PEG10*) are characteristic markers of VCTs that are involved in trophoblast proliferation and placental formation[27]. Genes involved in producing key pregnancy hormones, such as *CYP19A1* (encoding the estrogen-producing enzyme aromatase) and *CGA* (encoding human chorionic gonadotropin), are specifically expressed in SCTs[28,29]. SCTs represent the primary source of placental estrogen, as evidenced by the expression of essential estrogen synthesis genes such as *CYP19A1* and *HSD17B1*[30,31]. Further investigation of these gene functions may facilitate the identification of placental biomarkers associated with FGR in EOPE.

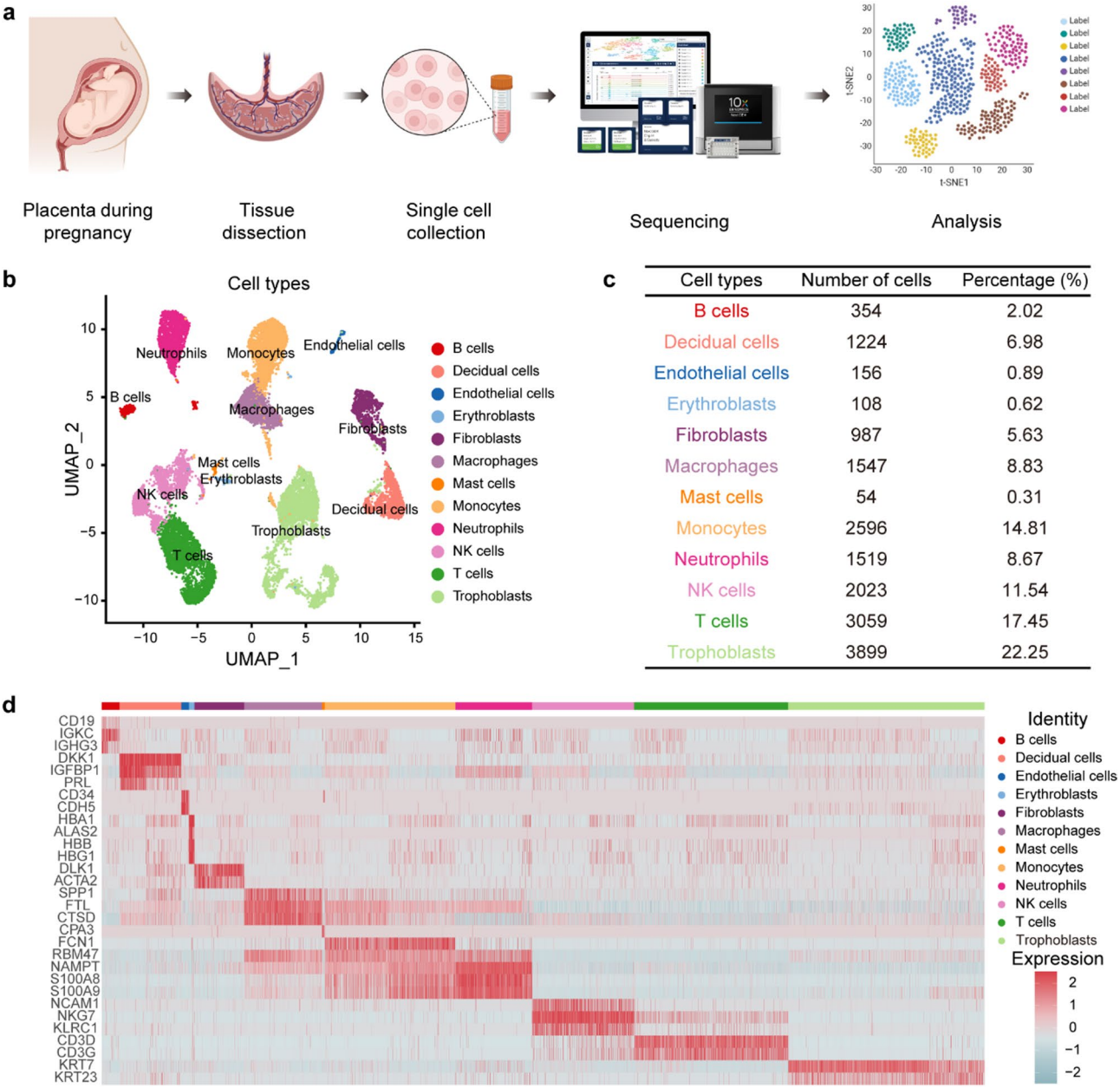

Fig. 1. Single-cell transcriptomic profiling and dissection of cellular heterogeneity in human placenta. **a** Workflow for primary placental samples for scRNA-seq. **b-c** Main cell clusters in placental tissue are demonstrated using UMAP plots, with cells colored and labeled based on their respective gene expression profiles. Cell numbers and percentages for each major cluster are shown in the right panel. Specific gene markers used for cell cluster identification are provided in Supplementary Table S1. **d** Heatmap generated based on expression levels of specific marker genes in each cluster. (Images in Fig. 1a were created using https://biorender.com/.)

Characterization of *HSD17B1* downregulation in SCTs

Building on the identification of SCT-specific estrogen-related genes described above, we next focused on HSD17B1 to determine whether its altered expression contributed to the reduced estrogen levels observed in patients with EOPE. To characterize the molecular landscape of estrogen-associated gene expression across diverse placental trophoblast subtypes, we employed VlnPlot and FeaturePlot for detailed analysis of gene expression profiles (Fig. 3a, b). Among these, *HSD17B1* was highly enriched in SCTs. This gene encodes 17β-hydroxysteroid dehydrogenase type 1, an enzyme essential for converting estrone, a less potent form of estrogen, into the more biologically active estradiol. Estradiol is key to maintaining placental function and supporting healthy pregnancies[32]. In EOPE-affected placentas, reduced HSD17B1 expression was observed in conjunction with lower estrogen-related gene expression levels, indicating alterations in the normal placental hormone synthesis profile.

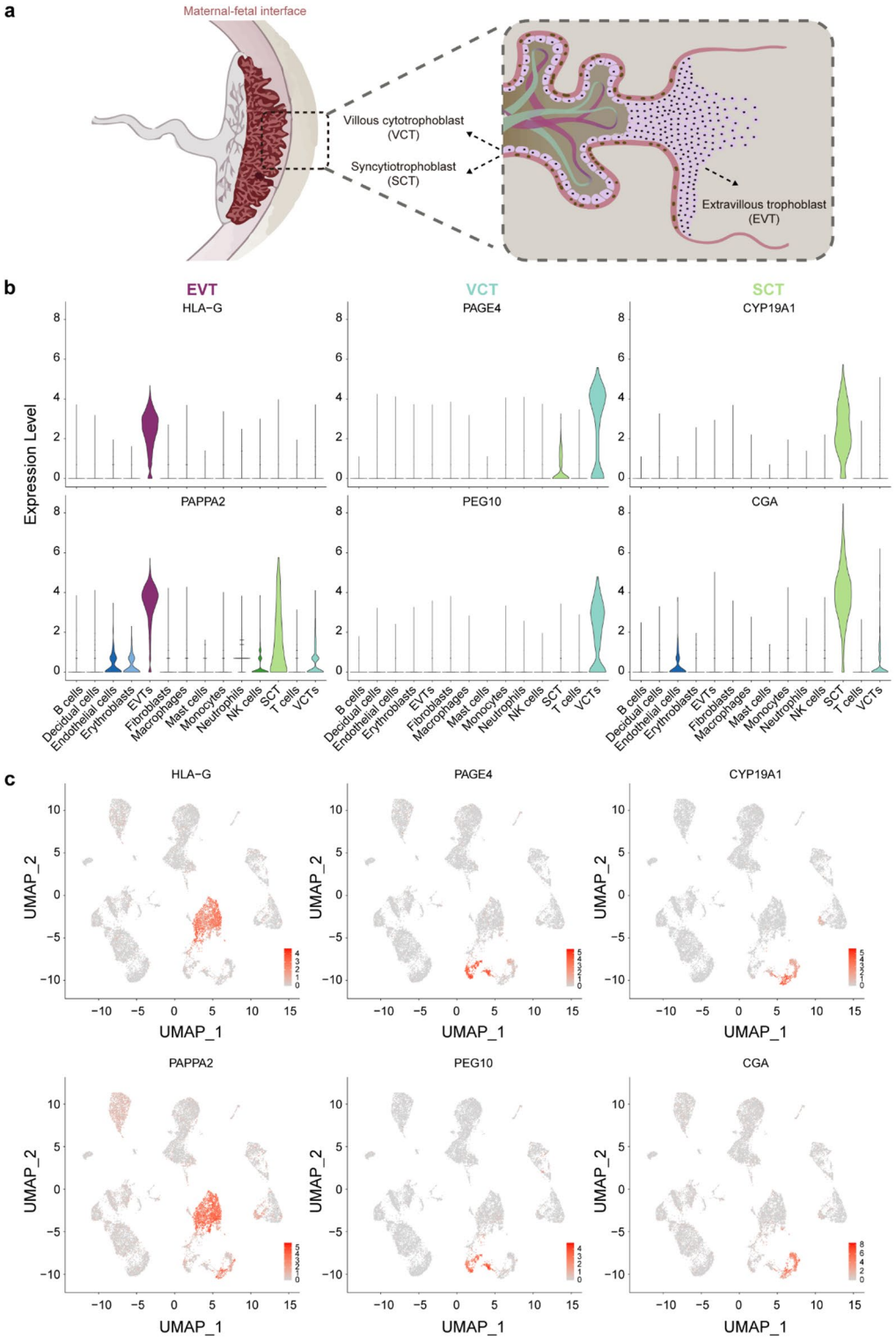

Fig. 2. Expression levels of specific marker genes of diverse trophoblast subtypes examined using scRNA-seq analysis. **a** Diagram illustrating the maternal–fetal interface during pregnancy. **b** Violin plots showing expression levels of representative markers for each trophoblast subtype within each cluster. **c** Expression levels of representative markers for each trophoblast subtype visualized on a UMAP plot. Color scale from gray to red indicates relative expression levels from low to high.

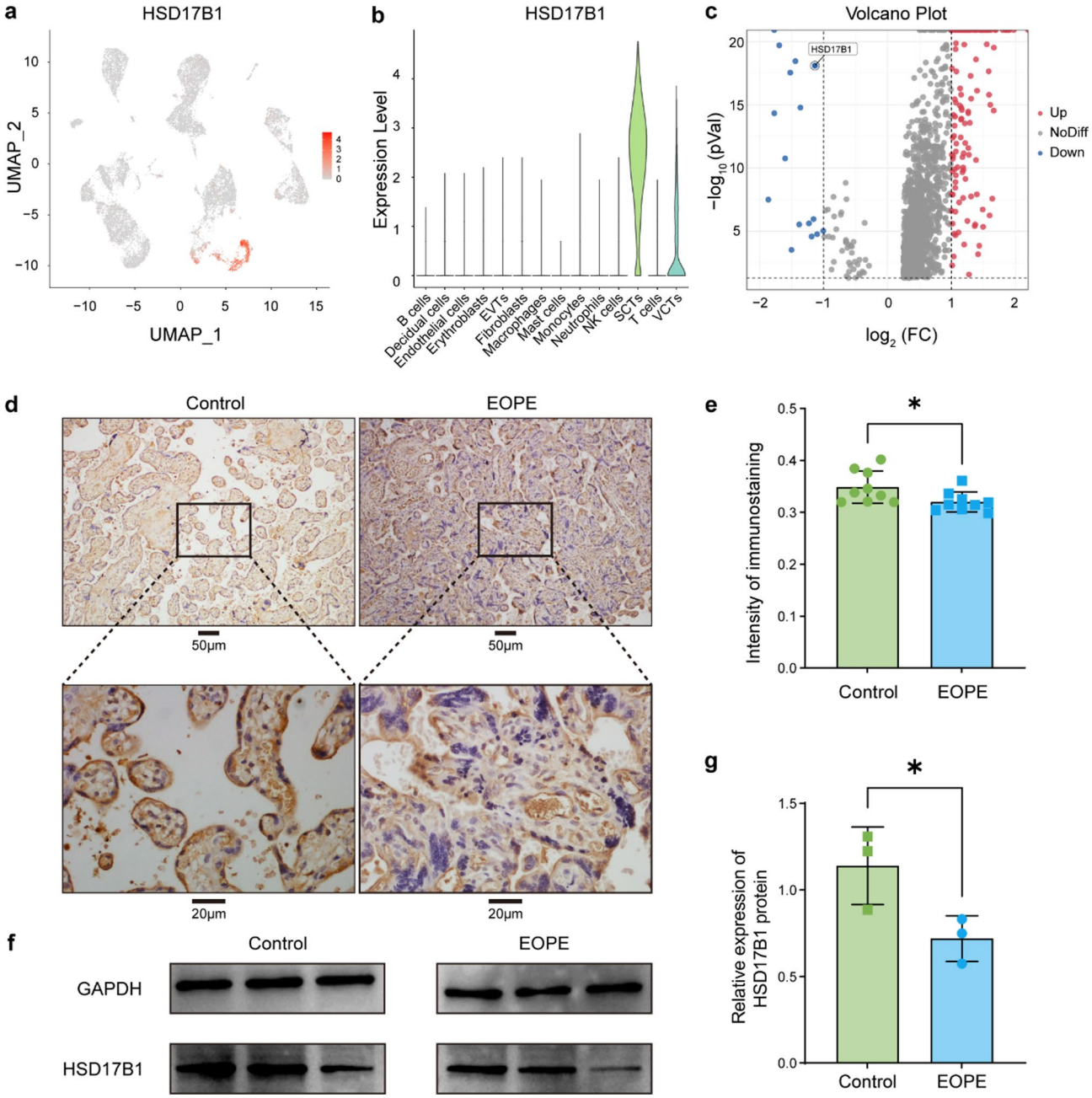

Fig. 3. Analysis of HSD17B1 gene in scRNA-seq and placental tissues from patients with EOPE and healthy controls. **a** Expression levels of HSD17B1 visualized on a UMAP plot. Color scale from gray to red indicates relative expression levels from low to high. **b** Violin plots displaying expression of HSD17B1 across all cell types identified in placental tissue. **c** Volcano plots showing the distribution of DEGs between patients with EOPE and healthy controls. Red spots represent upregulated genes, blue spots indicate downregulated genes, and gray spots indicate no significant expression change. **d** Representative IHC staining of placental tissue sections for HSD17B1 in SCTs from healthy pregnant women (left) and patients with EOPE (right). **e** Quantification of IHC showing reduced HSD17B1 expression in EOPE-affected placentas ($n = 3$). **f**, **g** Western blotting (**f**) and quantification (**g**) of HSD17B1 levels in placental samples from healthy pregnant women and EOPE patients ($n = 3$). Data shown as mean (SD); unpaired t-test, $^*p = 0.0311$.

To evaluate the impact of disease status on gene expression, we compared the levels of key genes associated with estrogen secretion in SCTs from the placentas of patients with EOPE with those from healthy controls. A total of 1,419 DEGs were identified, with 1,358 upregulated and 61 downregulated genes (Supplementary Table S2). As shown in the volcano plot, the expression of HSD17B1 was significantly downregulated in the SCTs of EOPE-affected placental tissues (Fig. 3c).

To validate the reduced expression of *HSD17B1* as a potential biomarker of EOPE, we assessed its expression in placental tissues. We performed immunohistochemical (IHC) staining of placental samples using an anti-HSD17B1 antibody (Fig. 3d). Placental samples were obtained from both the EOPE and healthy control groups, with three samples per group and three randomly selected regions from each tissue section (Supplementary Fig. S1). Differences in the staining intensity revealed significantly lower expression levels of HSD17B1 in the SCTs of EOPE-affected placental tissues (Fig. 3e). These results were further validated by western blotting analysis (Fig. 3f, g and Supplementary Fig. S2).

Disproportionate trophoblast subtype distribution in EOPE

To understand the disproportionate distribution of trophoblast subtypes in EOPE further and their potential link to reduced estrogen secretion via SCTs, we analyzed the relative abundance of these cell populations in healthy placental samples and those from patients with EOPE. Compared with healthy placentas, we observed a decreased proportion of SCTs and an increased proportion of EVTs and VCTs in the placentas of patients with EOPE (Fig. 4a). To validate these findings further, we collected placental tissue samples from four patients with EOPE with FGR and four healthy pregnant women. We then analyzed the expression of Syncytin-1 in the SCT subpopulation using flow cytometry. Syncytin-1, an envelope protein of the HERV-W family, is specifically expressed in placental SCTs. Our results indicated that the proportion of SCTs within the trophoblast subpopulations was lower in the EOPE group than in the healthy control group, consistent with our scRNA-seq findings (Fig. 4b, c). Based on these observations, we hypothesized that trophoblast differentiation is disrupted in patients with EOPE. In patients with EOPE, the differentiation of VCTs into SCTs appears to be inhibited, increasing the proportion of VCTs and EVTs and decreasing the proportion of SCTs.

Pseudotime trajectory analysis of trophoblast differentiation in EOPE

To verify our hypothesis and explore the disruption of trophoblast differentiation in EOPE-affected placentas, we performed a pseudotime trajectory analysis using placental trophoblasts (Fig. 5a, b). In this analysis, the VCTs were positioned at the starting point, and the SCTs and EVTs were located at the two branches of the trajectory. Our analysis of gene expression dynamics along the differentiation trajectory enabled the identification of key genes essential for trophoblast differentiation (Supplementary Table S3). We compared the genes involved in VCT-to-SCT differentiation with DEGs in SCTs between the healthy and EOPE groups, revealing 1,351 pivotal genes (Fig. 5c). Our analysis highlighted the substantial downregulation of significant genes, including *CSH2*, *CSH1*, *CSHL1*, *KISS1*, *HOPX*, *LGALS14*, *HBA2*, and *HSD17B1* (Fig. 5d). The significantly reduced expression of

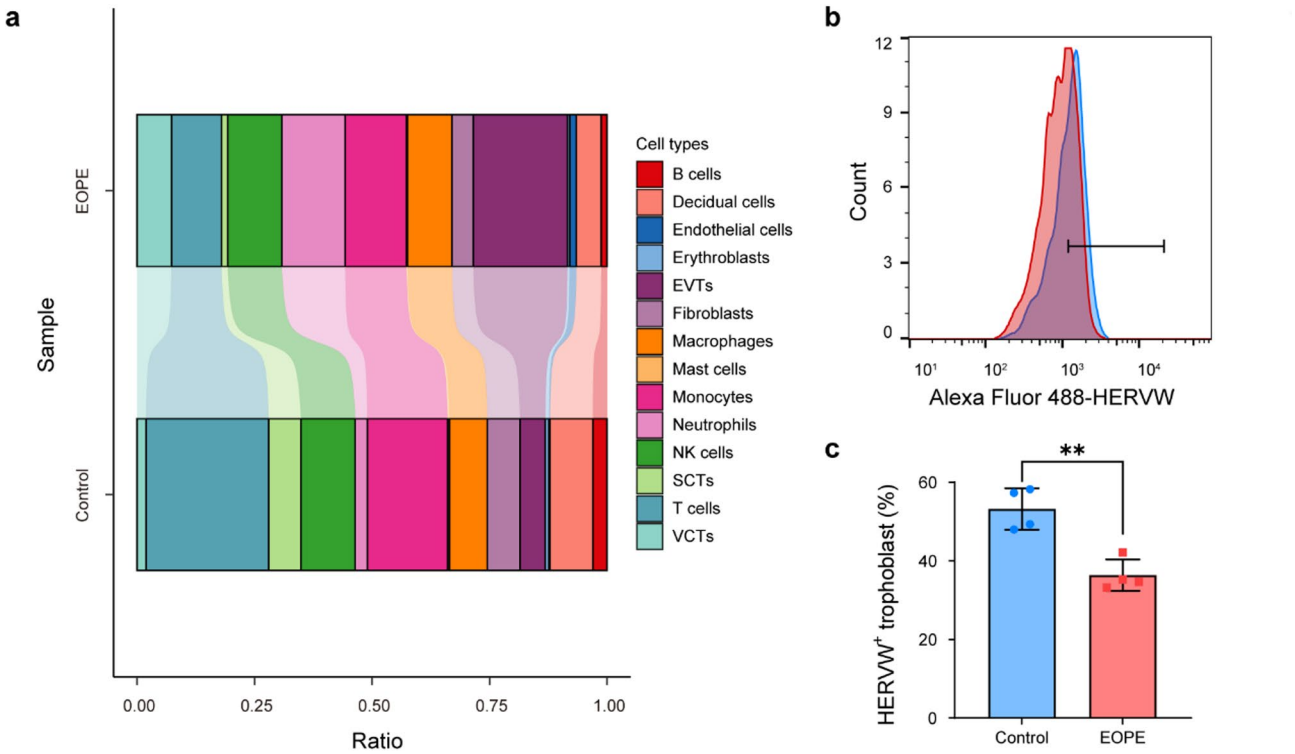

Fig. 4. Analysis of SCTs from patients with EOPE and healthy pregnant women using scRNA-seq and flow cytometry. **a** Column chart showing the proportion of each trophoblast type in EOPE and healthy pregnancy groups. **b** Flow cytometry analysis of placental trophoblasts from EOPE and healthy pregnancy groups. Histogram showing the percentage of HERVW + cells. **c** Comparison of proportions of trophoblasts expressing Syncytin-1 (HERVW) between EOPE and healthy pregnancy groups ($n = 4$). Data shown as mean (SD); unpaired *t*-test, $^{**}p = 0.0022$.

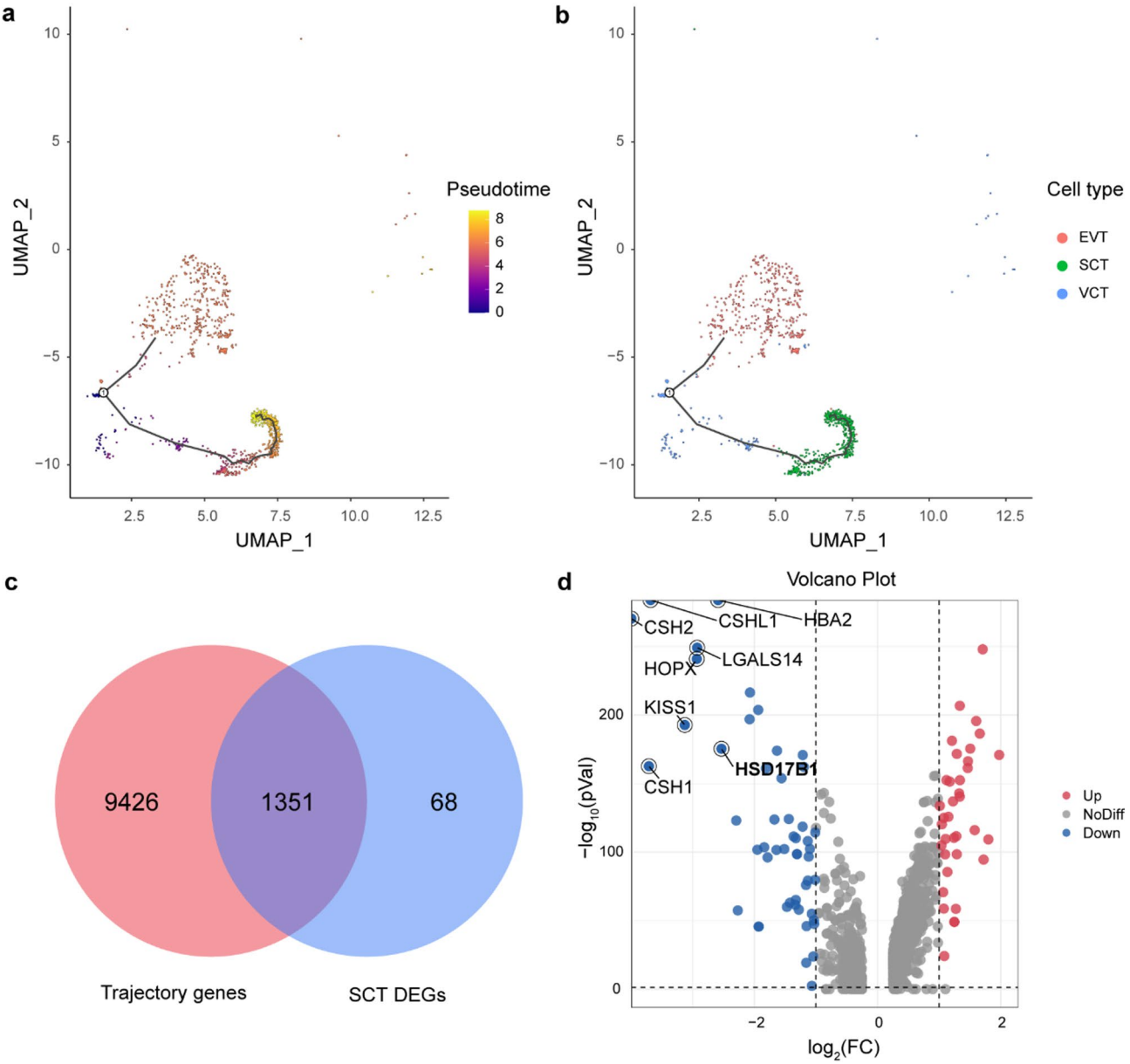

Fig. 5. Pseudotime trajectory and gene expression analysis of trophoblast differentiation. **a** Monocle3 visualization of pseudotime is colored in gradient from dark purple (start of pseudotime) to light yellow (end of pseudotime). **b** Pseudotime trajectory of trophoblasts from VCTs through EVTs and SCTs. Colors correspond to cell types, with red, green, and blue indicating EVT, SCT, and VCT cells, respectively. **c** Venn diagram illustrating the intersection of genes that vary along the differentiation trajectory from VCTs to SCTs with those differentially expressed genes between SCTs in EOPE and healthy groups. **d** Volcano plot displaying distribution and expression levels of intersecting genes, as identified in Fig. 5c, highlighting key regulators in trophoblast differentiation affected by EOPE.

the estrogen-related gene *HSD17B1* during EOPE progression suggests that it plays a critical role in trophoblast differentiation. The reduced *HSD17B1* expression in EOPE-affected placentas likely perturbs trophoblast lineage differentiation, skewing cell fate away from SCTs and toward VCTs and EVTs—a shift consistent with competitive differentiation from a common progenitor[33].

HSD17B1 as a key regulator of trophoblast differentiation and SCT formation

Trophoblast differentiation is a tightly regulated process in which VCTs fuse to form SCTs or differentiate into EVTs. Disruptions in trophoblast differentiation, particularly SCT formation, are prominent in patients with EOPE[5]. SCTs, a multinucleated cell layer, form through syncytialization and are vital for nutrient and gas exchange between the mother and fetus[34]. The human choriocarcinoma BeWo cell line is commonly used as a trophoblast and can undergo syncytialization through the action of forskolin (FSK), a cAMP pathway

activator[35]. This in vitro model mimics placental SCT formation observed during pregnancy[36]. To validate the function of HSD17B1 in trophoblast differentiation, we used siRNA to knock down HSD17B1 in BeWo cells. First, BeWo cells were transfected with an HSD17B1-targeting siRNA (siHSD17B1), and a non-targeting siRNA (siCont) was used as a parallel control. After transfection, the cells were treated with FSK to induce syncytialization. The effectiveness of HSD17B1 knockdown was confirmed at both the mRNA and protein levels (Fig. 6a, Supplementary Fig. S3). Subsequently, the impact on syncytialization was assessed by quantifying β-human chorionic gonadotropin (β-hCG) levels via qPCR, as β-hCG is a marker of trophoblast differentiation and SCT formation[37]. Chorionic gonadotropin subunit beta (CGB) mRNA levels represent β-hCG levels, and a reduction in β-hCG is often associated with impaired BeWo cell fusion and obstacles in SCT formation[38]. Our results demonstrated that HSD17B1 knockdown significantly reduced CGB mRNA levels, reflecting the production of β-hCG (Fig. 6b). In addition, CGB protein level was also downregulated following HSD17B1 knockdown (Supplementary Fig. S4). This reduction suggests that HSD17B1 suppression may affect BeWo cell fusion and SCT formation, implying that HSD17B1 may play a role in regulating trophoblast differentiation and that its downregulation may hinder SCT formation.

To investigate BeWo cell differentiation further, following HSD17B1 knockdown, flow cytometry was performed to quantify the percentage of Syncytin-1 (HERVW$^+$) cells, a specific marker of SCTs, during differentiation from VCTs[39]. This approach provides a robust indicator of SCT formation and enables a comprehensive evaluation of the effects of HSD17B1 suppression on trophoblast fusion and differentiation[40,41]. No significant differences were observed between untreated cells and those transfected with siCont (Fig. 6c). In contrast, a significant reduction in the proportion of HERVW$^+$ cells among the HSD17B1 knockdown BeWo cells was observed, with only 21.6% expressing Syncytin-1 compared to that in the untreated and siCont-transfected groups (Fig. 6d). Additionally, we assessed estrogen levels in the culture supernatants of BeWo cells from each treatment group using ELISA. Knocking down *HSD17B1* decreased estrogen levels in BeWo cell supernatants, and adding FSK did not significantly increase estrogen levels (Fig. 6e). Although BeWo cells differ from primary trophoblast cells, they serve as a viable in vitro substitute for studying placental trophoblast function[42–44]. These findings indicate that *HSD17B1* participates in regulating estrogen secretion and the differentiation of placental trophoblasts.

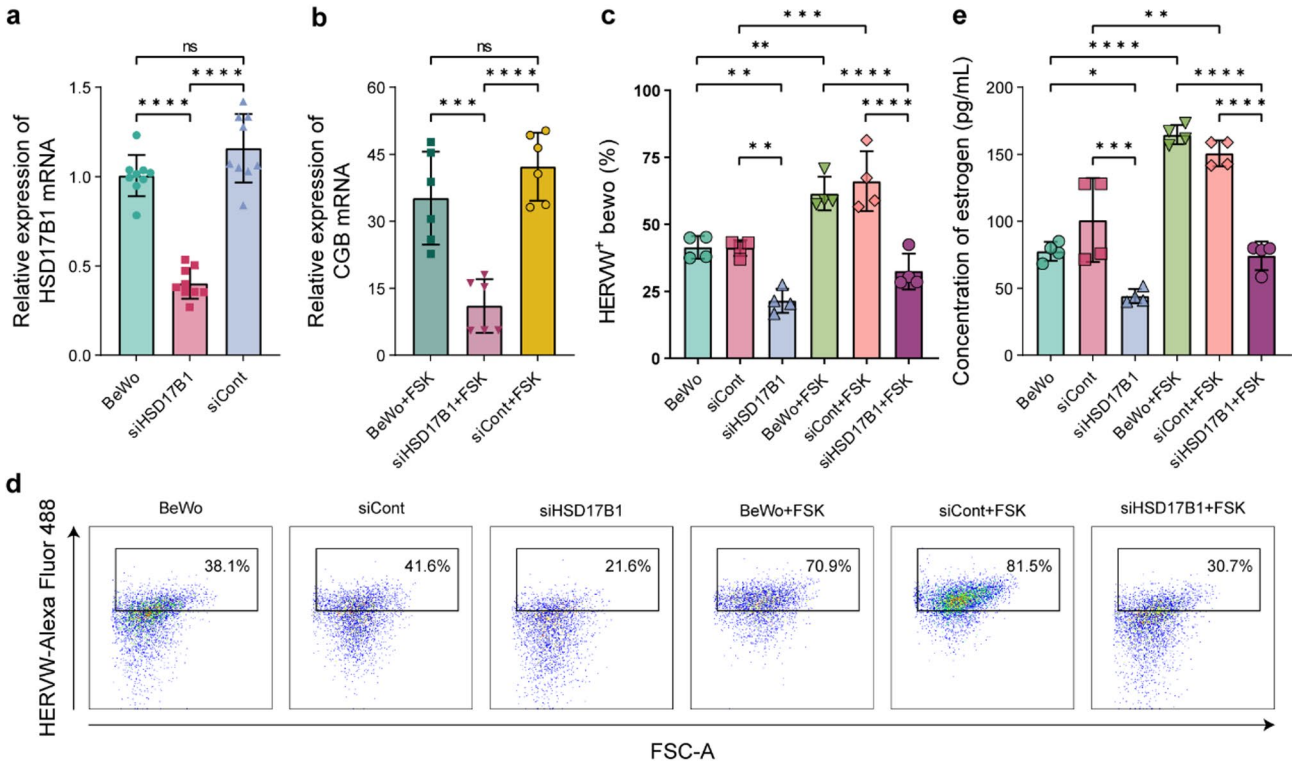

Fig. 6. Validation of syncytialization in HSD17B1 knockdown BeWo cells. **a** qPCR analysis of HSD17B1 mRNA levels in untreated BeWo cells and those transfected with siRNA ($n=9$). **b** qPCR analysis of CGB mRNA levels in untreated BeWo cells and those transfected with siRNA after FSK stimulation ($n=6$). **c** Comparison of percentages of Syncytin-1 (HERVW+)-expressing cells in BeWo cells following different treatments ($n=4$). **d** Flow cytometry analysis showing the percentage of Syncytin-1 (HERVW+)-expressing BeWo cells after different treatments ($n=4$). **e** Measurement of estrogen secretion in BeWo cells from each treatment group. Data shown as mean (SD); one-way ANOVA followed by Turkey's multiple comparison test, $^*p<0.05$, $^{**}p<0.01$, $^{***}p<0.001$, $^{****}p<0.0001$.

Discussion

Early-onset preeclampsia (EOPE) is a severe form of preeclampsia that contributes to life-threatening maternal vascular complications and fetal morbidities, with placental dysfunction serving as the primary pathogenic mediator. Our findings reveal the molecular mechanisms linking estrogen downregulation with impaired trophoblast differentiation in EOPE with FGR. Based on our scRNA-seq analysis of placental tissues derived from patients with EOPE-FGR, we identified HSD17B1, a key estradiol synthase gene, as the pivotal regulatory node, the downregulation of which promotes both placental hypoestrogenism and the arrest of SCT differentiation (Fig. 7). Further confirmation based on IHC and western blotting analysis revealed significantly reduced HSD17B1 expression in the SCT of EOPE-affected placentas compared with that in healthy controls, thereby providing evidence for its role in the pathophysiology of EOPE.

To mechanistically determine the pathophysiological role of HSD17B1, we established BeWo trophoblast models in vitro recapitulating EOPE-associated cellular behavior, using which we demonstrated that the knockdown of HSD17B1 resulted in a pronounced reduction in 17β-estradiol biosynthesis and disrupted SCT formation, as evidenced by reductions in Syncytin-1 (HERVW^{+}) cell populations and the secretion of estrogen. This dual defect of impaired SCT differentiation coupled with SCT-associated gene network suppression contributes to fundamental maldevelopment of the placenta.

SCTs constitute the outermost layer of placental villi and serve as a functional conduit for maternal–fetal exchange, including gaseous exchange, nutrient uptake, and waste elimination. This structural–functional imperative is further exemplified by the polarized expression of nutrient transporters and angiogenic regulators in SCTs, which collectively sustain fetal development[45,46]. Our findings are consistent with emerging evidence indicating that impaired SCT formation, manifested as syncytial layer thinning and dysfunction and placental surface area reduction, disrupts placental vascular modeling and nutrient and oxygen exchange capacities, thereby generating a hypoxic/nutrient-deprived environment that directly promotes FGR progression while further impairing EVT invasion and migration[47].

Anatomical deterioration correlated with SCT dysfunction, mirroring the HSD17B1-depleted signature identified in our trophoblast models. These mechanistic links between defective trophoblast differentiation, impaired SCT formation, and the arrest of estrogen biosynthesis define EOPE-FGR as a placental endocrine developmental disorder and identify HSD17B1 potentiation as a potential dual-axis therapeutic strategy for rescuing SCT differentiation and restoring estrogen signaling pathways.

Conclusions

In this study, based on integrated scRNA-seq analyses and cell model assessment, we succeeded in establishing HSD17B1 as a central regulatory node in the pathogenesis of EOPE. Our scRNA-seq analysis of placental trophoblasts in EOPE-FGR specimens enabled us to identify HSD17B1 as a representative downregulated gene within SCT subpopulations, which was confirmed using immunohistochemical analyses of clinical specimens. Furthermore, a complementary BeWo cell model, in which HSD17B1 was knocked down, confirmed that HSD17B1 orchestrates both estrogen biosynthesis and SCT differentiation. On the basis of these findings, we identified HSD17B1 as the molecular linker between trophoblast competence and estrogen homeostasis in EOPE, which could lay the foundation for developing placenta-centric precision medicine, from risk prediction methods to targeted therapies mitigating the maternal–fetal mortality cascade in EOPE.

Methods

Sample collection

This study was performed in line with the principles of the Declaration of Helsinki and was approved by the Institutional Ethics Committee of the First Hospital of Jilin University (approval number 2024-HS-145).

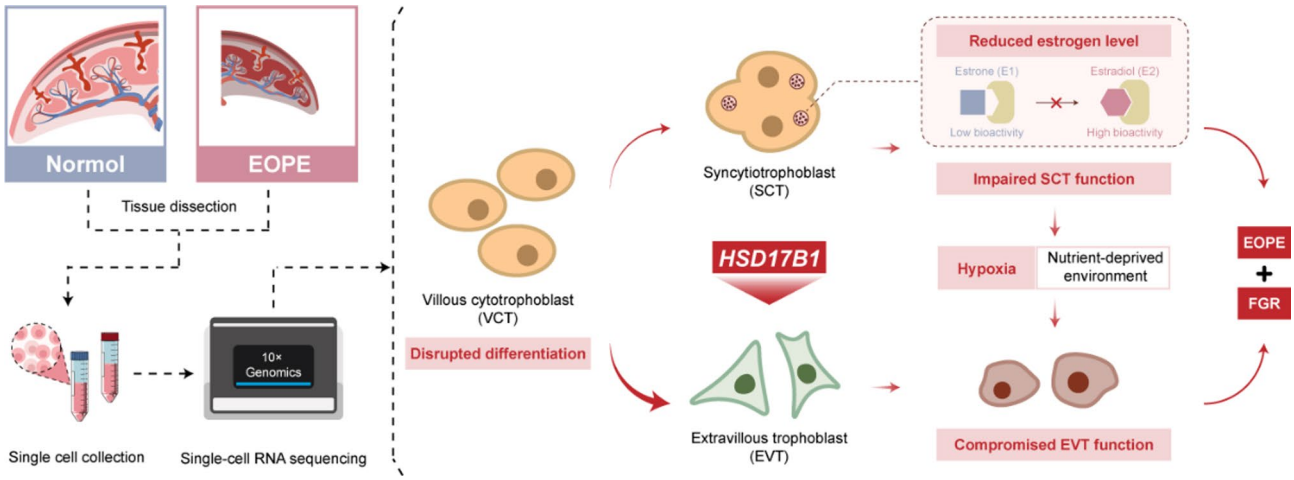

Fig. 7. Schematic model illustrating how HSD17B1 downregulation leads to abnormal trophoblast differentiation and dysfunction in EOPE.

Written informed consent was obtained from all participants after the nature and possible consequences of the study were explained. Preeclampsia patients were diagnosed in strict accordance with the American College of Obstetricians and Gynecologists (ACOG) guidelines[48], with EOPE defined as diagnosis before 34 weeks of gestation. Both EOPE patients and age- and body mass index (BMI)-matched healthy pregnant women (free of any comorbidities) were recruited from the Department of Obstetrics at the First Hospital of Jilin University. Detailed clinical information is provided in Supplementary Tables S4 and S5. We specifically selected patients with EOPE who delivered between 24 and 33 + 6 weeks of gestation. One of the recruited patients diagnosed with FGR presented at 31 + 4 weeks of gestation, whereas ultrasound estimated the gestational age at 27 + 4 weeks; this sample was used for scRNA-seq. Only patients who were not in active labor and were scheduled for cesarean section were included to avoid cellular contamination from the birth canal and to ensure placental cellular viability.

Single-cell suspension preparation

For placental parenchymal biopsy after delivery, 1 cm^3 of fresh placental tissue was dissected from a region 2 cm deep and 5 cm away from the umbilical cord insertion after peeling the fetal membranes. The dissected tissues were washed in phosphate-buffered saline (PBS) and subjected to enzymatic digestion in 1640 medium containing collagenase IV (1 ng/mL) and DNase I (2 μg/mL). Red blood cells were lysed and removed using Red Blood Cell Lysis Buffer (R1010, Solarbio, Beijing, China). Dead cells were removed using a Dead Cell Removal Kit (130-090-101, Miltenyi Biotec, Bergisch Gladbach, Germany), and the single-cell suspension was washed again in PBS. Successful dissociation was confirmed using CountStar (Countstar BioTech) cell analysis.

Single-cell RNA sequencing and data processing

A single-cell suspension was loaded onto a Chromium Controller (10× Genomics). The cDNA library was prepared according to the manufacturer's instructions (Chromium Next GEM Single Cell 3′ GEM, Library & Gel Bead Kit V3.1) and sequenced on an Illumina NovaSeq 6000 instrument using a 150-bp paired-end strategy, aiming for over 150 gigabases per sample[19]. Raw sequencing data were processed using the Cell Ranger pipeline (version 7.0.1) and aligned to the human reference genome GRCh38. Gene-barcode matrices containing barcoded cells and gene expression counts were imported into the Seurat R toolkit (version 4.1.1)[49,50]. Cells with a small library size (number of reads < 200) or a high mitochondrial transcript ratio (> 0.4) and genes expressed in fewer than three cells were excluded. Gene expression matrices were normalized and standardized for the remaining cells using the R package Seurat[51]. Gene expression matrices from different samples were then integrated, and batch effects were removed by canonical correlation analysis and mutual nearest neighbor anchors using the Seurat package[50].

Identification of cell types and marker genes

Highly variable genes were extracted for PCA, and 22 significant principal components were used for cluster analysis. Clusters were visualized using UMAP. Cell type identities were determined based on the expression of known markers in the Cell Marker database and the Single R package (version 2.0.0)[52]. Marker genes were identified by running Seurat FindMarkers at normalized expression levels. Additionally, significant marker genes (false discovery rate [FDR] $p < 0.05$) were narrowed down with the criteria of expressing cell percentage > 0.25 and $\log_2$ fold change > 0. The top ten marker genes were selected according to the fold change and difference in the percentage of cells expressing the gene.

Differentially expressed gene analysis

We compared gene expression between trophoblasts from EOPE-affected placentas and healthy pregnant women using the same method as that used for identifying cell marker genes. Differentially expressed genes (DEGs) were defined by FDR $p < 0.05$ and $\log_2$ fold change > 0.25 or < − 0.25[53]. The SCT-transformed data from the Seurat pipeline were used for the heatmap, feature plots, and violin plots.

Pseudotime trajectory analysis

The DEGs of the VCTs, SCTs, and EVTs were identified using Seurat. The expression levels of genes in at least 10 cells were analyzed using the Monocle3 R package (version 1.3.4)[54].

Immunohistochemistry

Paraffin-embedded human placental tissues were deparaffinized and rehydrated. The sections were then incubated with 3% H_2O_2 to block endogenous peroxidase activity. Tissue sections were incubated overnight at 4 °C with rabbit anti-HSD17B1 antibody (1 μg/mL; PA5-79400, Invitrogen, California, US), followed by a 50-min incubation with HRP-conjugated goat anti-rabbit IgG (SA00001-2, Proteintech, Wuhan, China). The sections were then subjected to a diaminobenzidine chromogen reaction, counterstained with hematoxylin, differentiated, blued, dehydrated, cleared, and air-dried. The results were visualized using bright-field microscopy.

Cell culture

Human choriocarcinoma BeWo cells were purchased from ProCell (CL-0500, Wuhan, China). BeWo cells were cultured in Ham's F-12 K (Kaighn's) medium (21-127-022, Gibco, New York, USA) and Dulbecco's modified Eagle medium (11965092, Gibco) supplemented with 15% fetal bovine serum (FS401-02, Transgene Biotech, Beijing, China), penicillin (100 U/mL), and streptomycin (100 mg/mL) at 37 °C in 5% CO_2 and 95% air. Exponential-phase cells were subcultured in six-well plastic culture flasks and cultured for 24 h to 50% confluence. Cells in the siRNA groups were transfected with siRNA for 48 h, whereas those in the control groups were cultured without transfection.

Name of siRNA	Sense (5′–3′)	Antisense (5′–3′)
HSD17B1 siRNA	GUGGGUGGCUAAUUAAGAUTT	AUCUUAAUUAGCCACCCACTT
Control siRNA	UUCUCCGAACGUGUCACGUTT	ACGUGACACGUUCGGAGAATT

Table 1. Sequence of double-stranded SiRNA targeting HSD17B1.

Name of primers	Forward primer (5′–3′)	Reverse primer (5′–3′)
HSD17B1	GGCTGCCTTTCAATGACGTTT	ACTCGATCAGGCTCAAGTGGAC
CGB	GTGTGCATCACCGTCAACAC	GGTAGTTGCACACCACCTGA
GAPDH	TCAAGGCTGAGAACGGGAAG	CGCCCCACTTGATTTTGGAG

Table 2. Sequences of primers used in this study.

SiRNAs and transfection

The target, sense, and antisense sequences are listed in Table 1. All siRNA duplexes were synthesized by Jilin Comate Biotech Company (Comate Biosciences Co., Jilin, China) and reconstituted in nuclease-free water to a concentration of 10 μM. Cells were transfected with HSD17B1 or Scrambled HSD17B1 siRNA (100 nM) using Lipofectamine 2000 DNA transfection reagent (11668019, Invitrogen) according to the manufacturer's protocol by incubating cells for 6 h. Forskolin or vehicle (dimethyl sulfoxide) was then added to a final concentration of 10 mM, followed by further incubation for 48 h at 37 °C. At the end of the incubation period, cell viability exceeded 95%, as assessed using the trypan blue exclusion assay. Cultures were conducted in triplicate for each set of experiments to assess reproducibility.

Flow cytometry

BeWo and human placental trophoblasts were analyzed using flow cytometry. BeWo cells were labeled with HERV antibody (PA5-79220, Invitrogen) for 30 min at 4 °C, washed three times, labeled with Goat Anti-Rabbit IgG H&L (Alexa Fluor® 488) (ab150077, Abcam, Cambridge, UK) for 20 min at 4 °C in the dark, and again washed three times. For flow cytometry analysis of placental cells, the staining steps mentioned above were performed. Cells were then fixed with BD Cytofix/Cytoperm solution (554722, BD Biosciences, NJ, USA) at 4 °C for 20 min, washed twice in BD Perm/Wash buffer, and incubated with Alexa Fluor® 647 Anti-Cytokeratin 7 antibody (ab192077, Abcam) at 4 °C for 30 min. The cells were washed twice with BD Perm/Wash buffer and resuspended for flow cytometry analysis. Cells were acquired using a Cytek Aurora spectral cytometer and analyzed using FlowJo 10.8.1 software.

Quantitative polymerase chain reaction (qPCR)

Total RNA was extracted using a FastPure Cell/Tissue Total RNA Isolation Kit Version 2 (Vazyme, Nanjing, China). RNA was reverse-transcribed using HiScript II Q RT SuperMix for qPCR (+gDNA wiper). The qPCR assay was performed using ChamQ Universal SYBR qPCR Master Mix on an Applied Biosystems QuantStudio 3&5 Real-time PCR System (Thermo Fisher Scientific). Expression data were normalized to GAPDH mRNA expression levels. Data were calculated using the $\mathbf{2}^{-\Delta\Delta Ct}$ method[55]. The primer sequences are shown in Table 2.

Western blotting

Protein samples were isolated from tissues or cells using RIPA lysis buffer (R0010, Solarbio), and protein concentration in the supernatant was measured using the BCA Protein Assay Kit (PC0020, Solarbio). Prior to electrophoresis, samples were denatured by boiling at 100 °C for 10 min, after which 50 μg of total protein from each sample was loaded onto 4-20% precast gels (DG101-01-V2, Transgene Biotech) for sodium dodecyl sulfate-polyacrylamide gel electrophoresis. After electrophoresis, proteins were transferred from the gel to a polyvinylidene fluoride (PVDF) membrane. The membrane was incubated in blocking buffer diluted in Tris-buffered saline containing 0.1% Tween-20 (TBST) at room temperature for 60 min with agitation. Following blocking, the PVDF membrane was washed, incubated overnight at 4 °C with rabbit anti-HSD17B1 antibody (PA5-79400, Invitrogen) or rabbit anti-CG beta antibody (CPA1220, Cohesion Biosciences, Suzhou, China) diluted 1:1000 in blocking buffer, washed again, and incubated for 1 h at room temperature with HRP-conjugated goat anti-rabbit IgG (SA00001-2, Proteintech). The membrane was then washed with TBST and incubated with ECL reagent solution (36208ES76, Yeasen Biotechnology, Shanghai, China). The protein band density of the western blots was quantified by measuring the gray-scale values of the target protein relative to α-Tubulin (CPA6383, Cohesion Biosciences) using ImageJ (National Institutes of Health, Bethesda, MD, USA).

ELISA for semi-quantitative detection of Estrogen

The estradiol concentrations in the supernatants of BeWo cells transfected with HSD17B1 siRNA, Scrambled HSD17B1 siRNA, or untransfected controls were measured using an Estradiol ELISA kit (E-OSEL-H0005, Elabscience, Wuhan, China). ELISA was performed according to the manufacturer's instructions, and all samples were assayed in triplicate. The inter-assay variability was less than 10%.

Statistical analysis

Data are expressed as means ± standard deviation (SD). Statistical analyses were performed using two-tailed Student's *t*-test to determine the significance of the differences between two groups. One-way ANOVA with Dunnett's multiple comparison test was used to compare the differences among multiple groups. Statistical analysis was performed using Prism 9 (GraphPad, San Diego, CA, USA), and statistical significance is indicated in the figures ($^{*}p < 0.05$, $^{**}p < 0.01$, $^{***}p < 0.001$). Statistical significance was set at $p < 0.05$.

Data availability

The datasets used and analyzed during this study are available from the corresponding author on reasonable request. Raw sequencing data and processed gene expression data have been deposited in the Gene Expression Omnibus (GEO) databank under accession numbers GSE282038 for the EOPE sample (available at the following URL: https://www.ncbi.nlm.nih.gov/geo/query/acc.cgi? acc=GSE282038) and GSE267340 for the control sampl e (available at the following URL: https://www.ncbi.nlm.nih.gov/geo/query/acc.cgi? acc=GSE267340).

Received: 14 February 2025; Accepted: 13 May 2025
Published online: 20 May 2025

References

1. Marzioni, D. et al. Importance of STAT3 signaling in preeclampsia (Review). *Int. J. Mol. Med.* **55**, 58. https://doi.org/10.3892/ijmm.2025.5499 (2025).
2. Annesi, L., Tossetta, G., Borghi, C. & Piani, F. The role of Xanthine oxidase in pregnancy complications: A systematic review. *Antioxidants* **13**, 1234 (2024).
3. Piani, F. et al. Serum uric acid to creatinine ratio and risk of preeclampsia and adverse pregnancy outcomes. *J. Hypertens.* **41**, 1333–1338. https://doi.org/10.1097/hjh.0000000000003472 (2023).
4. Soliman, Y. et al. Respiratory outcomes of late preterm infants of mothers with early and late onset preeclampsia. *J. Perinatol.* **40**, 39–45. https://doi.org/10.1038/s41372-019-0497-4 (2020).
5. Sheridan, M. A. et al. Early onset preeclampsia in a model for human placental trophoblast. *Proc. Natl. Acad. Sci.* **116**, 4336–4345. (2019). https://doi.org/10.1073/pnas.1816150116
6. Takahashi, M. et al. Fetal growth restriction as the initial finding of preeclampsia is a clinical predictor of maternal and neonatal prognoses: A single-center retrospective study. *BMC Pregnancy Childbirth.* **21**, 678. https://doi.org/10.1186/s12884-021-04152-2 (2021).
7. Feng, W. & Luo, Y. Preeclampsia and its prediction: Traditional versus contemporary predictive methods. *J. Maternal-Fetal Neonatal Med.* **37**, 2388171. https://doi.org/10.1080/14767058.2024.2388171 (2024).
8. Robillard, P. Y., Dekker, G., Scioscia, M. & Saito, S. Progress in the understanding of the pathophysiology of immunologic maladaptation related to early-onset preeclampsia and metabolic syndrome related to late-onset preeclampsia. *Am. J. Obstet. Gynecol.* **226**, S867–S875. https://doi.org/10.1016/j.ajog.2021.11.019 (2022).
9. Berkane, N. et al. From pregnancy to preeclampsia: A key role for estrogens. *Endocr. Rev.* **38**, 123–144. https://doi.org/10.1210/er.2016-1065 (2017).
10. Shao, X. et al. Testosterone represses Estrogen signaling by upregulating miR-22. *Hypertension* **69**, 721–730. https://doi.org/10.1161/HYPERTENSIONAHA.116.08468 (2017).
11. Heinosalo, T., Saarinen, N. & Poutanen, M. Role of hydroxysteroid (17beta) dehydrogenase type 1 in reproductive tissues and hormone-dependent diseases. *Mol. Cell. Endocrinol.* **489**, 9–31. https://doi.org/10.1016/j.mce.2018.08.004 (2019).
12. Hakkarainen, J. et al. Hydroxysteroid (17β)-dehydrogenase 1-deficient female mice present with normal puberty onset but are severely subfertile due to a defect in luteinization and progesterone production. *FASEB J.* **29**, 3806–3816. https://doi.org/10.1096/fj.14-269035 (2015).
13. He, W., Gauri, M., Li, T., Wang, R. & Lin, S. X. Current knowledge of the multifunctional 17β-hydroxysteroid dehydrogenase type 1 (HSD17B1). *Gene* **588**, 54–61. https://doi.org/10.1016/j.gene.2016.04.031 (2016).
14. Hilborn, E., Stål, O. & Jansson, A. Estrogen and androgen-converting enzymes 17β-hydroxysteroid dehydrogenase and their involvement in cancer: With a special focus on 17β-hydroxysteroid dehydrogenase type 1, 2, and breast cancer. *Oncotarget* **8** (2017).
15. Bamodu, O. A. et al. Differential but concerted expression of HSD17B2, HSD17B3, SHBG and SRD5A1 testosterone tetrad modulate therapy response and susceptibility to disease relapse in patients with prostate Cancer. *Cancers* **13**, 3478 (2021).
16. Cornel, K. M. C., Bongers, M. Y., Kruitwagen, R. P. F. M. & Romano, A. Local Estrogen metabolism (intracrinology) in endometrial cancer: A systematic review. *Mol. Cell. Endocrinol.* **489**, 45–65. https://doi.org/10.1016/j.mce.2018.10.004 (2019).
17. Wan, J. et al. The reduction in circulating levels of Estrogen and progesterone in women with preeclampsia. *Pregnancy Hypertens.* **11**, 18–25. https://doi.org/10.1016/j.preghy.2017.12.003 (2018).
18. Guo, L. et al. Differentially expressed MicroRNAs and affected biological pathways revealed by modulated modularity clustering (MMC) analysis of human preeclamptic and IUGR placentas. *Placenta* **34**, 599–605. https://doi.org/10.1016/j.placenta.2013.04.007 (2013).
19. Zheng, G. X. Y. et al. Massively parallel digital transcriptional profiling of single cells. *Nat. Commun.* **8**, 14049. https://doi.org/10.1038/ncomms14049 (2017).
20. Maltepe, E., Fisher, S. J. & Placenta the forgotten organ. *Annu. Rev. Cell Dev. Biol.* **31**, 523–552. https://doi.org/10.1146/annurev-cellbio-100814-125620 (2015).
21. Arechavaleta-Velasco, F., Koi, H., Strauss, J. F. & Parry, S. Viral infection of the trophoblast: Time to take a serious look at its role in abnormal implantation and placentation? *J. Reprod. Immunol.* **55**, 113–121. https://doi.org/10.1016/S0165-0378(01)00143-7 (2002).
22. Murphy, V. E., Smith, R., Giles, W. B. & Clifton, V. L. Endocrine regulation of human fetal growth: The role of the mother, placenta, and fetus. *Endocr. Rev.* **27**, 141–169. https://doi.org/10.1210/er.2005-0011 (2006).
23. Burton, G. J. & Jauniaux, E. The cytotrophoblastic shell and complications of pregnancy. *Placenta* **60**, 134–139. https://doi.org/10.1016/j.placenta.2017.06.007 (2017).
24. Velicky, P. et al. Genome amplification and cellular senescence are hallmarks of human placenta development. *PLoS Genet.* **14**, e1007698. https://doi.org/10.1371/journal.pgen.1007698 (2018).
25. Djurisic, S. & Hviid, T. V. F. HLA class Ib molecules and immune cells in pregnancy and preeclampsia. *Front. Immunol.* **5** https://doi.org/10.3389/fimmu.2014.00652 (2014).
26. Handschuh, K. et al. Modulation of PAPP-A expression by PPARγ in human first trimester trophoblast. *Placenta* **27**, 127–134. https://doi.org/10.1016/j.placenta.2005.10.012 (2006).
27. Zhou, W. et al. Trophoblast cell subtypes and dysfunction in the placenta of individuals with preeclampsia revealed by single-Cell RNA sequencing. *Mol. Cells.* **45**, 317–328. https://doi.org/10.14348/molcells.2021.0211 (2022).

28. Kamat, A., Graves, K. H., Smith, M. E., Richardson, J. A. & Mendelson, C. R. A 500-bp region, approximately 40 kb upstream of the human CYP19 (aromatase) gene, mediates placenta-specific expression in transgenic mice. *Proc. Natl. Acad. Sci. U.S.A.* **96 8**, 4575–4580 (1999).
29. Toda, K., Simpson, E. R., Mendelson, C. R., Shizuta, Y. & Kilgore, M. W. Expression of the gene encoding aromatase cytochrome P450 (CYP19) in fetal tissues. *Mol. Endocrinol.* **8**, 210–217. https://doi.org/10.1210/mend.8.2.8170477 (1994).
30. Hill, M. et al. Steroid metabolome in fetal and maternal body fluids in human late pregnancy. *J. Steroid Biochem. Mol. Biol.* **122**, 114–132. https://doi.org/10.1016/j.jsbmb.2010.05.007 (2010).
31. Strauss, J. F. & FitzGerald, G. A. in *Yen and Jaffe's Reproductive Endocrinology (Eighth Edition)* (eds Jerome F. Strauss & Robert L. Barbieri) 75–114.e117 (Elsevier, 2019).
32. Mazza, C., Breton, R., Housset, D. & Fontecilla-Camps, J. C. Unusual charge stabilization of NADP < sup>+ in 17β-Hydroxysteroid Dehydrogenase *. *J. Biol. Chem.* **273**, 8145–8152. https://doi.org/10.1074/jbc.273.14.8145 (1998).
33. Yi, C. et al. TBX3 reciprocally controls key trophoblast lineage decisions in villi during human placenta development in the first trimester. *Int. J. Biol. Macromol.* **263**, 130220. https://doi.org/10.1016/j.ijbiomac.2024.130220 (2024).
34. Renaud, S. J. & Jeyarajah, M. J. How trophoblasts fuse: An in-depth look into placental syncytiotrophoblast formation. *Cell. Mol. Life Sci.* **79**, 433. https://doi.org/10.1007/s00018-022-04475-z (2022).
35. Gauster, M., Moser, G., Orendi, K. & Huppertz, B. Factors involved in regulating trophoblast fusion: Potential role in the development of preeclampsia. *Placenta* **30**, 49–54. https://doi.org/10.1016/j.placenta.2008.10.011 (2009).
36. Zheng, R. et al. Deep RNA sequencing analysis of syncytialization-related genes during bewo cell fusion. *Reproduction* **153**, 35–48. https://doi.org/10.1530/rep-16-0343 (2017).
37. Mansilla, M., Wang, Y., Lim, R., Palmer, K. & Nie, G. HtrA4 is up-regulated during trophoblast syncytialization and bewo cells fail to syncytialize without HtrA4. *Sci. Rep.* **11**, 14363. https://doi.org/10.1038/s41598-021-93520-1 (2021).
38. Cocquebert, M. et al. Comparative expression of hCG β-genes in human trophoblast from early and late first-trimester placentas. *Am. J. Physiol.-Endocrinol. Metab.* **303**, E950–E958. https://doi.org/10.1152/ajpendo.00087.2012 (2012).
39. Costa, M. A. Scrutinising the regulators of syncytialization and their expression in pregnancy-related conditions. *Mol. Cell. Endocrinol.* **420**, 180–193. https://doi.org/10.1016/j.mce.2015.11.010 (2016).
40. Lavillette, D. et al. The envelope glycoprotein of human endogenous retrovirus type W uses a divergent family of amino acid transporters/cell surface receptors. *J. Virol.* **76**, 6442–6452. https://doi.org/10.1128/jvi.76.13.6442-6452.2002 (2002).
41. Sugimoto, J., Sugimoto, M., Bernstein, H., Jinno, Y. & Schust D. A novel human endogenous retroviral protein inhibits cell-cell fusion. *Sci. Rep.* **3**, 1462. https://doi.org/10.1038/srep01462 (2013).
42. Vidal, M. S. Establishment and comparison of human term placenta–derived trophoblast cells†. *Biol. Reprod.* **110**, 950–970. https://doi.org/10.1093/biolre/ioae026 (2024).
43. Karahoda, R. et al. Revisiting steroidogenic pathways in the human placenta and primary human trophoblast cells. *Int. J. Mol. Sci.* **22**, 1704 (2021).
44. Li, X., Li, Z. H., Wang, Y. X. & Liu, T. H. A comprehensive review of human trophoblast fusion models: Recent developments and challenges. *Cell. Death Discov.* **9**, 372. https://doi.org/10.1038/s41420-023-01670-0 (2023).
45. Fuchs, R. & Ellinger, I. Endocytic and transcytotic processes in villous syncytiotrophoblast: Role in nutrient transport to the human fetus. *Traffic* **5**, 725–738. https://doi.org/10.1111/j.1600-0854.2004.00221.x (2004).
46. Wang, Y. N. et al. The role of syncytin in placental angiogenesis and fetal growth. *Front. Cell. Dev. Biol.* **10** https://doi.org/10.3389/fcell.2022.852561 (2022).
47. Sun, C. et al. The placenta in fetal growth restriction: What is going wrong? *Placenta* **96**, 10–18 (2020). https://doi.org/10.1016/j.placenta.2020.05.003
48. Gestational Hypertension and Preeclampsia. ACOG practice bulletin, number 222. *Obstet. Gynecol.* **135**, e237–e260. https://doi.org/10.1097/aog.0000000000003891 (2020).
49. Wolock, S. L., Lopez, R., Klein, A. M. & Scrublet computational identification of cell doublets in single-cell transcriptomic data. *Cell. Syst.* **8**, 281–291e289. https://doi.org/10.1016/j.cels.2018.11.005 (2019).
50. Stuart, T. et al. Comprehensive integration of single-cell data. *Cell* **177**, 1888–1902e1821. https://doi.org/10.1016/j.cell.2019.05.031 (2019).
51. Satija, R., Farrell, J. A., Gennert, D., Schier, A. F. & Regev, A. Spatial reconstruction of single-cell gene expression data. *Nat. Biotechnol.* **33**, 495–502. https://doi.org/10.1038/nbt.3192 (2015).
52. Zhang, X. et al. CellMarker: A manually curated resource of cell markers in human and mouse. *Nucleic Acids Res.* **47**, D721–D728. https://doi.org/10.1093/nar/gky900 (2018).
53. Butler, A., Hoffman, P., Smibert, P., Papalexi, E. & Satija, R. Integrating single-cell transcriptomic data across different conditions, technologies, and species. *Nat. Biotechnol.* **36**, 411–420. https://doi.org/10.1038/nbt.4096 (2018).
54. Trapnell, C. et al. The dynamics and regulators of cell fate decisions are revealed by pseudotemporal ordering of single cells. *Nat. Biotechnol.* **32**, 381–386. https://doi.org/10.1038/nbt.2859 (2014).
55. Livak, K. J. & Schmittgen, T. D. Analysis of relative gene expression data using real-time quantitative PCR and the 2− ΔΔCT method. *Methods* **25**, 402–408. https://doi.org/10.1006/meth.2001.1262 (2001).

Acknowledgements

The author thanks Dr. Aowen Tian, Dr. Miaoran Zhang, MD. Yuxin Liu, MD. Yunxiao Zhang and MD. Zhiguo Su for their assistance with data analysis. The author also expresses gratitude to the Transplantation Immunology Laboratory of the First Hospital of Jilin University.

Author contributions

C.S. and P.C. conceived the experiments and revised the manuscript. S.Z. collected the samples, analyzed the data, performed the experiments, and wrote the manuscript. W.F., Z.S., and L.P. analyzed the data. P.X. and H.S. collected the samples. J.H. and S.D. participated in the experimental design. All authors read and approved the final manuscript.

Funding

This study was financially supported by the Wu Jieping Medical Foundation (Grant No. 320.6750.2021-06-32), the Finance Department of Jilin Province, China (Grant No. JLSCZD2019-053), Natural Science Funds in the Science and Technology Department of Jilin Province, China (Grant No. 20210101295JC), and the Open Project of the Key Laboratory of Organ Regeneration and Transplantation, Ministry of Education (Grant No. 2020JC07).

Declarations

Competing interests
The authors declare no competing interests.

Additional information
Supplementary Information The online version contains supplementary material available at https://doi.org/10.1038/s41598-025-02490-1.

Correspondence and requests for materials should be addressed to P.C. or C.S.

Reprints and permissions information is available at www.nature.com/reprints.

Publisher's note Springer Nature remains neutral with regard to jurisdictional claims in published maps and institutional affiliations.